



## A simple and efficient eight node finite element for multilayer sandwich composite plates bending behavior analysis

Khmissi Belkaid, Nadir Boutasseta, Hamza Aouaichia, Djamel Eddine Gaagaia, Badreddine Boubir

Research Center in Industrial Technologies CRTI P.O.Box 64, Cheraga, Algeria

khmissi.belkaid85@gmail.com, n.boutasseta@crti.dz, h.aouaichia@crti.dz, d.gaagaia@crti.dz, b.boubir@crti.dz

Adel Deliou

University of Med Seddik Benyahia (UMSB of Jijel), Department of Mechanical Engineering Laboratory of Materials and Reactive Systems LMSR, University Djillali, Liabes, Sidi Bel-Abbes, Algeria.

del032003@yahoo.fr, adel.deliou@univ-jjel.dz, deliouadel15@gmail.com

**ABSTRACT.** In this paper, a  $C^0$  simple and efficient isoparametric eight-node element displacement-model based on higher order shear deformation theory is proposed for the bending behavior study of multilayer composites sandwich plates. Difficult  $C^1$ -continuity requirement is overcome efficiently by choosing seven degrees of freedom for each element node: two displacements for in-plane behavior and five bending unknowns namely: a transverse displacement, two rotations and two shear angles, which results in the approximation formulation having only first order derivative requirement. The governing equations of the element (constitutive, virtual work and equilibrium equations) are implemented for the prediction of approximate solutions of deflections and stresses of sandwich plates linear elastic problems. The formulation element is able to present a cubic in-plane displacement along both core and faces sandwich cross-sectional, as well as, the shear stresses are found to vary as quadratic field without requiring shear correction factors and independent from any transverse shear locking problems when the plate is thin. The accuracy and validity of the proposed formulation is verified through the numerical evaluation of displacements and stresses and their comparison with the available analytical 3D elasticity solutions and other published finite element results.

**KEYWORDS.** Third Order Shear Deformation Theory; Sandwich Composite Plates; Finite Element; Bending Behavior.



**Citation:** Belkaid, K., Boutasseta, N., Aouaichia, H., Gaagaia, D. E., Boubir, B., Deliou, A., A simple and efficient eight node finite element for multilayer sandwich composite plates bending behavior analysis, *Frattura ed Integrità Strutturale*, 61 (2022) 372-393.

**Received:** 27.03.2022

**Accepted:** 01.06.2022

**Online first:** 10.06.2022

**Published:** 01.07.2022

**Copyright:** © 2022 This is an open access article under the terms of the CC-BY 4.0, which permits unrestricted use, distribution, and reproduction in any medium, provided the original author and source are credited.



## INTRODUCTION

Sandwich composite plates are being increasingly used in many fields of modern technology due to their high strength, weight ratio and low maintenance cost. A good understanding of their behavior in terms of deformations and stresses distribution through the structures provide an effective vision for their applications.

Generally, sandwich composite structures are made-up of a very rigid isotropic or orthotropic face sheets and relatively soft thick core material. In mechanical analysis of the bending sandwich plate, displacement fields vary in a zigzag manner through the thickness, thus making the displacements very discontinuous at the layer interfaces due to the large variation in stress between layers. Hence, the development of a suitable computational theory is required for accurately predicting the responses of these laminated sandwich structures. In this context, a number of shear deformation theories have been developed in order to accurately model multilayer plate.

In the literature, the simplest equivalent single layer ESL laminate approach is the classical laminated plate theory (CLPT) Kirchhoff assumptions [1]. Their finite element model spatial approximations [2] contain C0-requirement for the in-plan displacements using Lagrange interpolation function, and transverse displacement C1-requirement using Hermite interpolation functions over the element. However, these elements models are characterized by a complex mathematical formulation due to the C1-requirement, and the theory is only appropriate for thin laminate plate analysis due to neglecting the effects of transverse shear deformation.

The simplest theory which takes into account the transverse shear deformation is the first order shear deformation theory [FSDT] [3, 4]. Their finite element models [5] are characterized by a simple formulation with C0-requirement for all degrees of freedom using Lagrange interpolation function. However, the theory requires shear correction factors and the transverse shear stresses show at least a quadratic distribution through the plate thickness according to Pagano three-dimensional elasticity theory [6].

Various analytical higher order theories (HSDT) have been proposed for the multilayer composite structures analysis, taking into account shear deformation effects without shear correction. Their kinematics assumption is expanded up to higher powers of the thickness coordinate and quadratic transverse shear [7-10]. Barut et al. [11] analyzed a thick sandwich plate by third and second order theories in which the in-plane and the transverse displacements show cubic and quadratic variations respectively through the thickness of the plate. Other analytical and experimental works can be found for the sandwich plate and shell analysis: Noor et al. [12], Kant et Swaminathan [13], Mantari et al. [14], Grover et al. [15], Kanematsu et al. [16], Torabizadeh and Fereidoon, [17], M. Michele et al. [18], Deliou Adel [19]. However, analytical methods are only suitable for specific simple boundary conditions and geometries. In this case, several (2D) finite element models based on higher order shear deformation theory (HSDT) have been developed [20] for the static analysis of multilayer composite sandwich plates.

B. Pandya , T. Kant [21] have presented a simple isoparametric finite element formulation based on a higher-order displacement model for flexure analysis of multilayer symmetric sandwich plates. B.S. Manjunatha, T. Kant [22] have evaluated the transverse stresses between layers of laminated composite and sandwich laminates using C0 nine and sixteen finite element formulation based on higher order theory. However, the models resort to use selective numerical integration scheme in order to overcome the shear locking problem. T. Kant and J. Kommineni, [23] presented a simple C0 quadrilateral Lagrange finite element formulation with nine-nodes and nine degrees of freedom per node based on refined higher-order shear deformation theory for the linear and geometrically non-linear analysis of fiber reinforced composite and sandwich plates. However, the selective integration scheme based on Gauss quadrature rules is introduced in order to overpass the shear locking problem. C.-P. Wu and C.-C. Lin [24] have presented the stress and displacement analysis of the thick sandwich plates using an interlaminar stress mixed nine-node finite element based on high order deformation theory. However, the formulation element possesses eleven nodal field variables in each node. R.P. Khandelwal et al. [25] have developed an efficient C0 continuous nine-node finite element model with eleven nodal field variables for each node based on combined theories refined higher order shear deformation theory (RHSDT) and least square error (LSE) method for the static analysis of soft core sandwich plates, the model satisfied the continuity of transverse shear stress condition between layer interfaces and zero transverse shear stress at the top and bottom of the sandwich plate. M.K. Pandit et al. [26] proposed a computationally efficient C0 nine-node finite element based on improved higher order zigzag theory for the static analysis of laminated sandwich plate with soft compressible core. However, the element has eleven nodal field variables for each node adopting a reduced integration technique for the evaluation of stiffness matrix. T.M. Tu , T.H. Quoc [27] have developed a nine-noded rectangular element with nine degrees of freedom at each node for the bending and vibration analysis of laminated and sandwich composite plates. The theory accounts for parabolic distribution of the transverse shear strains through the thickness of the plate and rotary inertia effects. A. Nayak et al. [28] analyzed the bending behavior of isotropic, laminated composite and sandwich plates using two C0 quadrilateral finite element formulations based on higher-



order theory where the element possess seven nodal field variables in each node. However, the formulations introduced assumed strain interpolations for the transverse shear strain in order to overcome the shear locking problem. Chalak et al. [29] presented an improved C0 2D nine-node finite element with eleven field variables per node. The model is based on higher order zigzag plate theory and has been applied to the analysis of laminated composites and sandwich plates. R. Sahoo and B. Singh [30] suggested an efficient C0 eight noded isoparametric element with seven degrees of freedom per node based on a new inverse trigonometric zigzag theory for the static analysis of laminated and sandwich plates. However, the selective integration scheme is used in order to solve the locking shear problem. According to this literature survey, HSDT finite element models impose inconvenients such as: large number of nodal field variables, often encounter a locking problem when the plate is thin and resort to impose stiffness penalty in the formulation to remedy this problem.

On the other hand, single layer Reddy's theory is one of the higher-order theories used most often for analyzing multilayer plates, being able to evaluate stresses and transverse shear strains with a small variables number, not depending on the number of layers [9]. However, Reddy's theory encounter formulation complications when the finite element requires C1 second-order derivatives. The same problem also arises in the classical theory of thin plates [31]. Therefore, many finite-element models (2D) based on Reddy's third order theory have been proposed in the literature [20] for the bending behavior analysis of isotropic and multilayer composite plates. Furthermore, Reddy finite elements usually use conforming and non-conforming formulation where the C1 transverse displacement and its derivatives are interpolated by a modified bicubic Hermite functions, while the in-plane displacement and shear rotations are interpolated C0 Lagrange functions (JN Reddy [32], Phan and Reddy [33], Averill and Reddy [34], J. Ren, . Hinton [35], Ine-Wei Liu [36])

The objective of this work is to propose an efficient plate bending elements based on Reddy's shear deformation theory, which has a simple formulation that overcome the difficult C1 requirement with small nodal field variables and that does not need to impose any stiffness penalty in the formulation and is also able to predict accurately the response of multilayer plates. Based on the recently proposed displacement-model [37], a serendipity isoparametric eight nodes finite element is formulated for the study of multilayer sandwich plate bending behavior. In the formulation of the element, seven nodal field variables are chosen in an efficient manner so that there is no need to impose any stiffness penalty and present simple mathematical formulation. In this work, the present sandwich plate element is used to solve many multilayer sandwich plates problems for various parameters such as, different loadings, geometry, boundary conditions, and materials.

## KINEMATICS

The displacement field of the plate according to Reddy's third order shear deformation theory (TSDT) [9] can be expressed as follows:

$$\begin{aligned}
 u_1 &= u + \zeta \psi_x - \frac{4\zeta^3}{3b} \left( \psi_x + \frac{\partial w}{\partial x} \right) \\
 u_2 &= v + \zeta \psi_y - \frac{4\zeta^3}{3b} \left( \psi_y + \frac{\partial w}{\partial y} \right) \\
 u_3 &= w
 \end{aligned} \tag{1}$$

where:  $u_1, u_2, u_3$  are the displacements field in the x, y and z directions respectively.

$u, v$  displacement of a point  $(x, y)$  on the mid-plane of the plate.  $\psi_x, \psi_y$  are rotations about the axes y and x respectively, and  $b$  is the thickness of the plate.

The strain associated with displacement field (1) are given as follows:

$$\begin{aligned}
 \epsilon_1 &= \frac{\partial u_1}{\partial x} = \epsilon_1^0 + \zeta (\kappa_1^0 + \zeta^2 \kappa_1^2) \\
 \epsilon_2 &= \frac{\partial u_2}{\partial y} = \epsilon_2^0 + \zeta (\kappa_2^0 + \zeta^2 \kappa_2^2)
 \end{aligned}$$



$$\varepsilon_3 = \frac{\partial u_3}{\partial \zeta} = 0 \tag{2}$$

$$\varepsilon_4 = \left( \frac{\partial u_2}{\partial \zeta} + \frac{\partial u_3}{\partial y} + \frac{\partial u_3}{\partial y} \frac{\partial u_3}{\partial \zeta} \right) = \varepsilon_4^0 + \zeta^2 \kappa_4^2$$

$$\varepsilon_5 = \left( \frac{\partial u_1}{\partial \zeta} + \frac{\partial u_3}{\partial x} + \frac{\partial u_3}{\partial x} \frac{\partial u_3}{\partial \zeta} \right) = \varepsilon_5^0 + \zeta^2 \kappa_5^2$$

$$\varepsilon_6 = \left( \frac{\partial u_1}{\partial y} + \frac{\partial u_2}{\partial x} + \frac{\partial u_3}{\partial x} \frac{\partial u_3}{\partial y} \right) = \varepsilon_6^0 + \zeta \left( \kappa_6^0 + \zeta^2 \kappa_6^2 \right)$$

where:

$$\varepsilon_1^0 = \frac{\partial u}{\partial x}; \kappa_1^0 = \frac{\partial \psi_x}{\partial x}; \kappa_1^2 = -\frac{4}{3b^2} \left( \frac{\partial \psi_x}{\partial x} + \frac{\partial^2 w}{\partial x^2} \right)$$

$$\varepsilon_2^0 = \frac{\partial u}{\partial y}; \kappa_2^0 = \frac{\partial \psi_y}{\partial y}; \kappa_2^2 = -\frac{4}{3b^2} \left( \frac{\partial \psi_y}{\partial y} + \frac{\partial^2 w}{\partial y^2} \right)$$

$$\varepsilon_4^0 = \psi_y + \frac{\partial w}{\partial y}; \kappa_4^2 = -\frac{4}{b^2} \left( \psi_y + \frac{\partial w}{\partial y} \right)$$

$$\varepsilon_5^0 = \psi_x + \frac{\partial w}{\partial x}; \kappa_5^2 = -\frac{4}{b^2} \left( \psi_x + \frac{\partial w}{\partial x} \right)$$

$$\varepsilon_6^0 = \frac{\partial u}{\partial y} + \frac{\partial v}{\partial x} + \frac{\partial w}{\partial x} \frac{\partial w}{\partial y}; \kappa_6^0 = \frac{\partial \psi_x}{\partial y} + \frac{\partial \psi_y}{\partial x};$$

$$\kappa_6^2 = -\frac{4}{3b^2} \left( \frac{\partial \psi_x}{\partial y} + \frac{\partial \psi_y}{\partial x} + 2 \frac{\partial^2 w}{\partial x \partial y} \right)$$

## CONSTITUTIVE EQUATIONS

The laminate is usually made of several orthotropic layers (Fig 1). Each layer must be transformed into the laminate coordinate system (x, y, z) [2]. The stress-strain relationship is given as:

$$\begin{Bmatrix} \sigma_{xx} \\ \sigma_{yy} \\ \sigma_{xy} \end{Bmatrix}_k = \begin{bmatrix} \bar{C}_{11} & \bar{C}_{12} & \bar{C}_{16} \\ \bar{C}_{12} & \bar{C}_{22} & \bar{C}_{26} \\ \bar{C}_{16} & \bar{C}_{26} & \bar{C}_{66} \end{bmatrix}_k \begin{Bmatrix} \varepsilon_{xx} \\ \varepsilon_{yy} \\ \varepsilon_{xy} \end{Bmatrix}_k; \begin{Bmatrix} \sigma_{xz} \\ \sigma_{yz} \end{Bmatrix}_k = \begin{bmatrix} \bar{C}_{44} & \bar{C}_{45} \\ \bar{C}_{45} & \bar{C}_{55} \end{bmatrix}_k \begin{Bmatrix} \varepsilon_{xz} \\ \varepsilon_{yz} \end{Bmatrix}_k \tag{3}$$

where  $\bar{C}_{ij}$  are the transformed material constants:

$$\begin{aligned} \bar{C}_{11} &= C_{11}c^4 + 2(C_{12} + 2C_{66})c^2s^2 + C_{22}s^4 \\ \bar{C}_{12} &= (C_{11} + C_{22} - 4C_{66})c^2s^2 + C_{12}(c^4 + s^4) \\ \bar{C}_{16} &= (C_{11}c^2 + (C_{12} + 2C_{66})(s^2 - c^2) - C_{22}s^2)cs \\ \bar{C}_{22} &= C_{11}s^4 + 2(C_{12} + 2C_{66})c^2s^2 + C_{22}c^4 \\ \bar{C}_{26} &= (C_{11}s^4 + (C_{12} + 2C_{66})(c^2 - s^2) - C_{22}c^4)cs \\ \bar{C}_{66} &= (C_{11} + C_{22} - 4C_{12})c^2s^2 + C_{66}(c^2 - s^2) \\ \bar{C}_{44} &= C_{44}c^2 + C_{55}s^2 \\ \bar{C}_{45} &= (C_{55} - C_{44})cs \\ \bar{C}_{55} &= C_{55}c^2 + C_{44}s^2 \end{aligned}$$

where  $c = \cos\theta$ ,  $s = \sin\theta$  and  $\theta$  is angle between global axis and local axis for each laminate layer.

$$C_{11} = \frac{E_1}{1 - \nu_{12}\nu_{21}}; C_{12} = \frac{\nu_{12}E_2}{1 - \nu_{12}\nu_{21}}; C_{22} = \frac{E_2}{1 - \nu_{12}\nu_{21}}; C_{66} = G_{12}; C_{55} = G_{13}; C_{44} = G_{23}$$

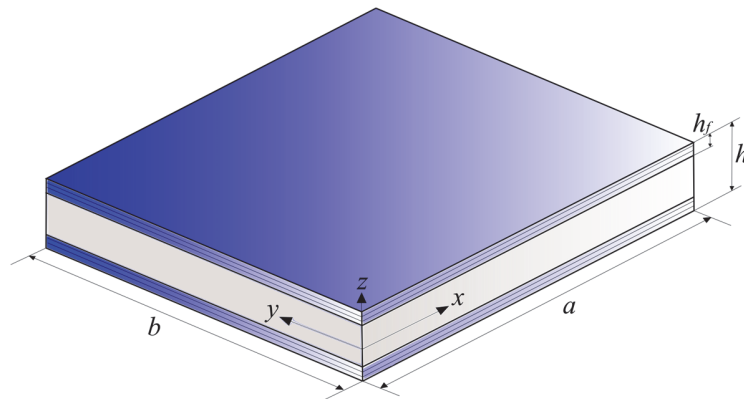


Figure 1: Geometry and coordinate system of the sandwich plate

The differential equilibrium equations for transverse stress analysis are given as follows [2]:

$$\begin{aligned} \sigma_{x\bar{z}} &= -\sum_{k=1}^n \int_{h_{k-1}}^{h_k} \left( \frac{\partial \sigma_{xx}^k}{\partial x} + \frac{\partial \sigma_{xy}^k}{\partial y} \right) d\bar{z} \\ \sigma_{y\bar{z}} &= -\sum_{k=1}^n \int_{h_{k-1}}^{h_k} \left( \frac{\partial \sigma_{xy}^k}{\partial x} + \frac{\partial \sigma_{yy}^k}{\partial y} \right) d\bar{z} \end{aligned} \tag{4}$$



**VIRTUAL WORK PRINCIPLE**

The static equations of the theory can be derived from the virtual work principle [9] by expressing the strain energy variation as follows:

$$\int_V (\sigma_{xx} \delta \varepsilon_{xx} + \sigma_{yy} \delta \varepsilon_{yy} + \sigma_{xy} \delta \varepsilon_{xy} + \sigma_{xz} \delta \varepsilon_{xz} + \sigma_{yz} \delta \varepsilon_{yz}) dV + \int_V q \delta W dV = 0 \tag{5}$$

According to the substitution of equations (2) in the static equation (5) we obtain:

$$\int_A \left[ N_{xx} \frac{\partial \delta u}{\partial x} + M_{xx} \frac{\partial \delta \psi_x}{\partial x} + P_{xx} \left( -\frac{4}{3b^2} \left( \frac{\partial \delta \psi_x}{\partial x} + \frac{\partial^2 \delta w}{\partial x^2} \right) \right) + N_{yy} \frac{\partial \delta v}{\partial y} + M_{yy} \frac{\partial \delta \psi_y}{\partial y} + P_{yy} \left( -\frac{4}{3b^2} \left( \frac{\partial \delta \psi_y}{\partial y} + \frac{\partial^2 \delta w}{\partial y^2} \right) \right) + N_{xy} \left( \frac{\partial \delta u}{\partial y} + \frac{\partial \delta v}{\partial x} \right) + M_{xy} \left( \frac{\partial \delta \psi_x}{\partial y} + \frac{\partial \delta \psi_y}{\partial x} \right) + P_{xy} \left( -\frac{4}{3b^2} \left( \frac{\partial \delta \psi_x}{\partial y} + \frac{\partial \delta \psi_y}{\partial x} + 2 \frac{\partial^2 \delta w}{\partial x \partial y} \right) \right) + Q_{xx} \left( \delta \psi_x + \frac{\partial \delta w}{\partial x} \right) + R_{xx} \left( -\frac{4}{b^2} \left( \delta \psi_x + \frac{\partial \delta w}{\partial x} \right) \right) + Q_{yy} \left( \delta \psi_y + \frac{\partial \delta w}{\partial y} \right) + R_{yy} \left( -\frac{4}{b^2} \left( \delta \psi_y + \frac{\partial \delta w}{\partial y} \right) \right) + q \delta W \right] dA = 0 \tag{6}$$

where the resultants forces are defined as follows:

$$\begin{bmatrix} N_{xx} & M_{xx} & P_{xx} \\ N_{yy} & M_{yy} & P_{yy} \\ N_{xy} & M_{xy} & P_{xy} \end{bmatrix} = \sum_{k=1}^n \int_{h_{k-1}}^{h_k} \begin{Bmatrix} \sigma_{xx} \\ \sigma_{yy} \\ \sigma_{xy} \end{Bmatrix} \left( 1, \tilde{x}, \tilde{x}^3 \right) d\tilde{x}; \quad \begin{bmatrix} Q_{xx} & R_{xx} \\ Q_{yy} & R_{yy} \end{bmatrix} = \sum_{k=1}^n \int_{h_{k-1}}^{h_k} \begin{Bmatrix} \sigma_{xz} \\ \sigma_{yz} \end{Bmatrix} \left( 1, \tilde{x}^2 \right) d\tilde{x} \tag{7}$$

Therefore, from the eq (7) and eq (3), we obtain the generalized relations resultants forces as follows [9]:

$$\begin{aligned} \begin{Bmatrix} \{N\} \\ \{M\} \\ \{P\} \end{Bmatrix} &= \begin{bmatrix} [A_{ij}] & [B_{ij}] & [E_{ij}] \\ sym & [D_{ij}] & [F_{ij}] \\ sym & sym & [H_{ij}] \end{bmatrix} \begin{Bmatrix} \varepsilon^0 \\ \kappa^0 \\ \kappa^2 \end{Bmatrix} \\ \begin{Bmatrix} \{Q\} \\ \{R\} \end{Bmatrix} &= \begin{bmatrix} [A_{ij}^s] & [D_{ij}^s] \\ sym & [F_{ij}^s] \end{bmatrix} \begin{Bmatrix} \{\gamma^s\} \\ \{\kappa^s\} \end{Bmatrix} \end{aligned} \tag{8}$$

where:

$$\begin{aligned} [\varepsilon_1^0 \quad \varepsilon_2^0 \quad \varepsilon_6^0 \quad \kappa_1^0 \quad \kappa_2^0 \quad \kappa_6^0 \quad \kappa_1^2 \quad \kappa_2^2 \quad \kappa_6^2]^T &= [\varepsilon^0 \quad \kappa^0 \quad \kappa^2]^T \\ [\varepsilon_4^0 \quad \varepsilon_5^0 \quad \kappa_4^2 \quad \kappa_5^2]^T &= [\gamma^s \quad \kappa^s]^T \\ (A_{ij}, B_{ij}, D_{ij}, E_{ij}, F_{ij}, H_{ij}) &= \sum_{k=1}^n \int_{h_{k-1}}^{h_k} \bar{C}_{ij} (1, \tilde{x}, \tilde{x}^2, \tilde{x}^3, \tilde{x}^4, \tilde{x}^6) d\tilde{x}, \quad i, j = 1, 2, 6 \\ (A_{ij}^s, D_{ij}^s, F_{ij}^s) &= \sum_{k=1}^n \int_{h_{k-1}}^{h_k} \bar{C}_{ij} (1, \tilde{x}^2, \tilde{x}^4) d\tilde{x}, \quad i, j = 4, 5 \end{aligned}$$



Substituting the resultant forces (8) in equation (6), the static equation becomes

$$\int_A (\delta \epsilon^{0T} [A] \epsilon^0 + \delta \epsilon^{0T} [B] \kappa^0 + \delta \epsilon^{0T} [E] \kappa^2 + \delta \kappa^{0T} [B] \epsilon^0 + \delta \kappa^{0T} [D] \kappa^0 + \delta \kappa^{0T} [F] \kappa^2 + \delta \kappa^{2T} [E] \epsilon^0 + \delta \kappa^{2T} [F] \kappa^0 + \delta \kappa^{2T} [H] \kappa^2 + \delta \gamma^{sT} [A^s] \gamma^s + \delta \gamma^{sT} [D^s] \kappa^s + \delta \kappa^{sT} [D^s] \gamma^s + \delta \kappa^{sT} [F^s] \kappa^s + q \delta w) dA = 0 \tag{9}$$

**FINITE ELEMENT FORMULATION**

In this work, a C0 isoparametric serendipity eight-node element (Fig.2) is employed for the bending analysis of sandwich plates based on Reddy’s third order shear deformation. In the present formulation element the complexities associated with C1 continuous plate are overcome with efficient manner by choosing seven nodal degrees of freedom (DOF) [37, 38] as follows: two displacements ( $u, v$ ) for the membrane behavior and five displacements ( $w, \psi_x, \psi_y, \theta_x, \theta_y$ ) for describing the bending behavior, where  $\theta_x = \left( \psi_x + \frac{\partial w}{\partial x} \right), \theta_y = \left( \psi_y + \frac{\partial w}{\partial y} \right)$  are shear angles.

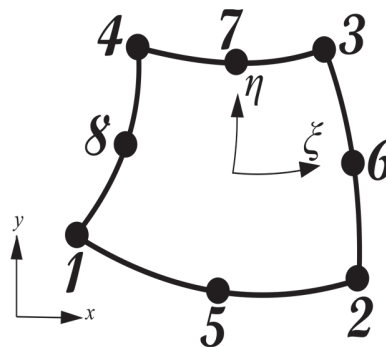


Figure 2: Eight-node isoparametric finite element

The generalized field variable and element geometry of the model at any point may be expressed in terms of nodal approximation as follows:

$$\begin{aligned} x(\xi, \eta) &= \sum_{i=1}^8 \bar{N}_i(\xi, \eta) x_i; \quad y(\xi, \eta) = \sum_{i=1}^8 \bar{N}_i(\xi, \eta) y_i \\ u(\xi, \eta) &= \sum_{i=1}^8 \bar{N}_i(\xi, \eta) u_i; \quad v(\xi, \eta) = \sum_{i=1}^8 \bar{N}_i(\xi, \eta) v_i; \quad \psi_x(\xi, \eta) = \sum_{i=1}^8 \bar{N}_i(\xi, \eta) \psi_{xi}; \quad \psi_y(\xi, \eta) = \sum_{i=1}^8 \bar{N}_i(\xi, \eta) \psi_{yi}; \\ \theta_x(\xi, \eta) &= \sum_{i=1}^8 \bar{N}_i(\xi, \eta) \theta_{xi}; \quad \theta_y(\xi, \eta) = \sum_{i=1}^8 \bar{N}_i(\xi, \eta) \theta_{yi} \end{aligned}$$

where corner nodes are defined as follows:

$$\bar{N}_i(\xi, \eta) = \frac{1}{4} (1 + \xi \xi_i) (1 + \eta \eta_i) (\xi \xi_i + \eta \eta_i - 1), i = 1, 2, 3, 4$$

and mid side nodes as:



$$\bar{N}_i(\xi, \eta) = \frac{1}{2}(1 - \xi^2)(1 + \eta\eta_i), i = 5, 7$$

$$\bar{N}_i(\xi, \eta) = \frac{1}{2}(1 - \xi\xi_i)(1 + \eta^2), i = 6, 8$$

$\bar{N}_i(\xi, \eta)$  are the bi-nonlinear interpolation functions of Lagrange type corresponding to node  $i=1-8$  [39].

The strain displacements vectors can be formed as derivative elementary nodal matrix  $[B]$  multiplied by the proposed nodal field variable  $\{\delta\}$  as follows:

$$\varepsilon^0 = [B_\varepsilon^0]\{\delta\}; \kappa^0 = [B_\kappa^0]\{\delta\}, \kappa^2 = [B_\kappa^2]\{\delta\}, \gamma^s = [B_\varepsilon^s]\{\delta\}, \kappa^s = [B_\kappa^s]\{\delta\} \tag{10}$$

$$[B_\varepsilon^0] = \begin{bmatrix} \bar{N}_{i,x} & 0 & 0 & 0 & 0 & 0 & 0 \\ 0 & \bar{N}_{i,y} & 0 & 0 & 0 & 0 & 0 \\ \bar{N}_{i,y} & \bar{N}_{i,x} & 0 & 0 & 0 & 0 & 0 \end{bmatrix}; [B_\kappa^0] = \begin{bmatrix} 0 & 0 & \bar{N}_{i,x} & 0 & 0 & 0 & 0 \\ 0 & 0 & 0 & \bar{N}_{i,y} & 0 & 0 & 0 \\ 0 & 0 & \bar{N}_{i,y} & \bar{N}_{i,x} & 0 & 0 & 0 \end{bmatrix}$$

$$[B_\kappa^2] = c_1 \begin{bmatrix} 0 & 0 & 0 & 0 & 0 & \bar{N}_{i,x} & 0 \\ 0 & 0 & 0 & 0 & 0 & 0 & \bar{N}_{i,y} \\ 0 & 0 & 0 & 0 & 0 & \bar{N}_{i,y} & \bar{N}_{i,x} \end{bmatrix}; [B_\varepsilon^s] = \begin{bmatrix} 0 & 0 & \bar{N}_{i,y} & 0 & \bar{N}_i & 0 & 0 \\ 0 & 0 & \bar{N}_{i,x} & \bar{N}_i & 0 & 0 & 0 \end{bmatrix}$$

$$[B_\kappa^s] = c_2 \begin{bmatrix} 0 & 0 & 0 & 0 & 0 & 0 & \bar{N}_i \\ 0 & 0 & 0 & 0 & 0 & \bar{N}_i & 0 \end{bmatrix}$$

$$\{\delta\}^T = \{u_i, v_i, w_i, \psi_{xi}, \psi_{yi}, \theta_{xi}, \theta_{yi}\}, i = 1-8$$

with:

$$c_1 = -4/3h^2, c_2 = -4/h^2$$

According to the substitution of strain matrix (10) in the static equation (9), the elementary stiffness matrix  $[K]_e$  is deduced according the static system  $[K]_e \{\delta\} = \{F\}$  [37] as follows:

$$[K]_e = \int_{-1}^1 \int_{-1}^1 ([B_\varepsilon^0]^T [A][B_\varepsilon^0] + [B_\varepsilon^0]^T [B][B_\kappa^0] + [B_\varepsilon^0]^T [E][B_\kappa^2] + [B_\kappa^0]^T [B][B_\varepsilon^0] + [B_\kappa^0]^T [D][B_\kappa^0] + [B_\kappa^0]^T [F][B_\kappa^2] + [B_\kappa^2]^T [E][B_\kappa^0] + [B_\kappa^2]^T [F][B_\kappa^0] + [B_\kappa^2]^T [H][B_\kappa^2] + [B_\varepsilon^s]^T [A^s][B_\varepsilon^s] + [B_\varepsilon^s]^T [D^s][B_\kappa^s] + [B_\kappa^s]^T [D^s][B_\varepsilon^s] + [B_\kappa^s]^T [F^s][B_\kappa^s]) \det[J] d\xi d\eta \tag{11}$$

where  $\{F\}, \{\delta\}$  are elementary nodal vectors of forces and degrees of freedom, respectively.

The analytical integration can be converted to Gauss's numerical integration [40]. Full integration scheme quadrature rules, namely (3x3) is employed in the energy expression for the evaluation of the element stiffness property.





**NUMERICAL EXAMPLES AND COMPARISON STUDIES**

In this section, several sandwich plates examples are solved to verify the effectiveness of the proposed formulation in the prediction of displacements and stresses results including different parameters such as, thickness ratios, materials, loading distribution, laminated face sheet, boundary conditions. The results of proposed model are compared with the three-dimensional elasticity solutions and other element models available in the literature.

*Bending of a simply supported sandwich square plate subject to a doubly sinusoidal transverse load*

For this example, the proposed element convergence and ability of the bending behavior is studied by considering a simply supported (f/c/f) symmetrical square sandwich plate subject to a doubly sinusoidal transverse load

$q(x, y) = q_0 \sin \frac{\pi x}{a} \sin \frac{\pi y}{b}$  for different thickness ratios  $a/h = 4, 10, 50, 100$ . The properties of the core and those of the sheets are shown in (Table 1). It is noted that normalized central deflection displacement results converge for different uniform mesh sizes toward Pagano 3D-elasticity solution [6] (Table 2). The increasing meshes indicate the accuracy and convergence rate of central transverse displacements results with a fast decrease of relative errors for both thin and moderately thick sandwich plates with no shear locking in the thin plates ( $a/h=50, 100$ ).

The simply supported boundary conditions used for the bending example are as follows:

$$x = \pm a/2 \rightarrow v = w = \psi_y = \theta_y = 0 ; y = \pm b/2 \rightarrow u = w = \psi_x = \theta_x = 0$$

The normalized deflection, stresses and in-plan are defined by:

$$\bar{w} = w \left( \frac{a}{2}, \frac{b}{2}, 0 \right) \left( \frac{b^3 E_2}{q_0 a^4} \right) 10^2, \bar{\sigma}_{xx} = \sigma_{xx} \left( \frac{a}{2}, \frac{b}{2}, \frac{b}{2} \right) \left( \frac{b^2}{q_0 a^2} \right), \bar{\sigma}_{yy} = \sigma_{yy} \left( \frac{a}{2}, \frac{b}{2}, \frac{b}{2} \right) \left( \frac{b^2}{q_0 a^2} \right),$$

$$\bar{\sigma}_{xy} = \sigma_{xy} \left( 0, 0, \frac{b}{2} \right) \left( \frac{b^2}{q_0 a^2} \right), \bar{\sigma}_{xz} = \sigma_{xz} \left( 0, \frac{b}{2}, 0 \right) \left( \frac{b}{q_0 a} \right), \bar{\sigma}_{yz} = \sigma_{yz} \left( \frac{a}{2}, 0, 0 \right) \left( \frac{b}{q_0 a} \right)$$

$$\bar{u} = u \left( \frac{100 b^3 E_2}{q_0 a^4} \right), \bar{v} = v \left( \frac{100 b^3 E_2}{q_0 a^4} \right)$$

| Proprieties    |       | E <sub>1</sub> | E <sub>2</sub> | G <sub>12</sub> | G <sub>13</sub> | G <sub>23</sub> | v <sub>12</sub> | Thickness |
|----------------|-------|----------------|----------------|-----------------|-----------------|-----------------|-----------------|-----------|
| Sandwich plate | Core  | 275.8 MPa      | 275.8 MPa      | 110.32 MPa      | 413.68 MPa      | 413.68 MPa      | 0.25            | 0.8h      |
|                | Sheet | 172369.9 MPa   | 6894.76 MPa    | 3447.38 MPa     | 1378.95 MPa     | 3447.38 MPa     | 0.25            | 0.1h      |

Table 1: Mechanical proprieties of a sandwich plate.

| Reference       | Theory   | $\bar{w} \left( \frac{a}{2}, \frac{b}{2}, 0 \right)$ |                 |                 |                 |
|-----------------|----------|--|-----------------|-----------------|-----------------|
|                 |          | a/h=4(err%)  | a/h=10(err %)   | a/h=50(err %)   | a/h=100(err %)  |
| Present (2×2)   | HSDT(Q8) | 6.5668 (13.55)                                       | 1.8739 (14.83)  | 0.60962 (34.78) | 0.3439 (61.43)  |
| Present (4×4)   |          | 7.1009 (6.52)  | 2.07035 (5.91)  | 0.91441 (2.181) | 0.8604 (3.5)    |
| Present (6×6)   |          | 7.1377 (6.03)  | 2.081172 (5.41) | 0.92644 (0.89)  | 0.8845 (0.796)  |
| Present (8×8)   |          | 7.1461 (5.927)                                       | 2.08326 (5.32)  | 0.92844 (0.68)  | 0.8888 (0.323)  |
| Present (10×10) |          | 7.1492 (5.88)  | 2.08396 (5.29)  | 0.92901 (0.61)  | 0.89005 (0.185) |
| Present (12×12) |          | 7.1508 (5.86)  | 2.08426 (5.27)  | 0.92923 (0.59)  | 0.89053 (0.131) |
| Pagano[6]       |          | Elasticity solution                                  | 7.5962          | 2.2004          | 0.9348          |

Table 2: Normalized center deflection convergence of a simply supported square sandwich plate subject to a doubly sinusoidal transverse load.



In Fig 3 the central normalized  $\bar{w}$  deflection is plotted for different  $a/h$  ratios. In Fig 4, the in-plane displacements  $u_1(a/2,0,0)$  and  $u_2(0,b/2,0)$  are described through the plate thickness as a cubic variation. It can be seen that the obtained bending responses by the present formulation are in excellent agreement with the elasticity solution of Pagano [6] and with those obtained by T. Kant and K. Swaminathan analytical solution [13].

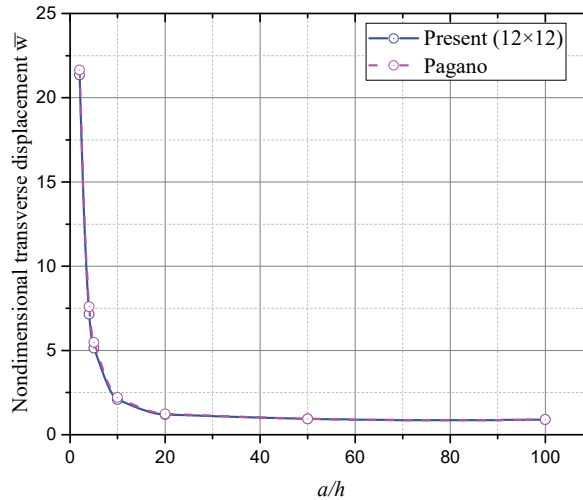


Figure 3: Evolution of normalized central transverse deflection  $\bar{w}$  with aspect ratio  $a/h$  of a simply supported sandwich plate ( $0^\circ / C / 0^\circ$ ) subject to a doubly sinusoidal transverse load.

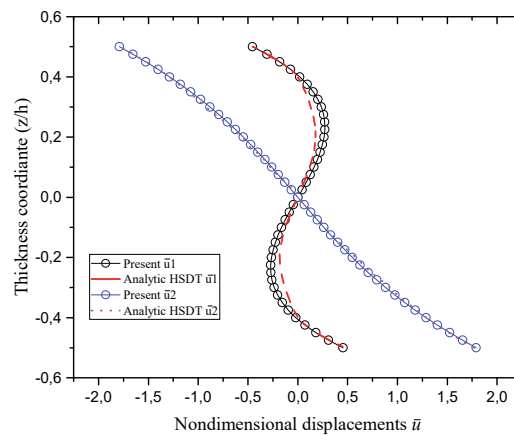


Figure 4: Evolution of normalized in-plane displacements  $\bar{u}_1, \bar{u}_2$  as function of the thickness of a simply supported ( $0^\circ / C / 0^\circ$ ) sandwich plate subject to a doubly sinusoidal transverse load  $a/h=4$ .

In Table 3, the bending sandwich plate ( $0^\circ / C / 0^\circ$ ) is studied for different aspect ratios  $a/h$  in order to present the normalized transverse deflection and maximum stresses using the constitutive equation. Furthermore, the transverse shear stresses are evaluated using the equilibrium equations. A close agreement has been found between the obtained results by the proposed element and those obtained using Pagano elasticity-3D solution [6], as well as with those obtained by finite element models based on different theories.

Furthermore, it's noting that in thin sandwich plate cases ( $a/h=50,100$ ), the results of the proposed model do not have locking shear problems with additional better accuracy in comparison with other model elements that have used stiffness penalty with a high number of nodal variables than the proposed model (e.g. B. Pandya, T. Kant [21], T. Kant and J. Kommineni, [23], M.K. Pandit et al. [26], Chalak et al. [29], R. Sahoo and B. Singh [30]).



| a/h | Reference                | Theory              | $\bar{w}$ | $\bar{\sigma}_{xx}$ | $\bar{\sigma}_{yy}$ | $\bar{\sigma}_{xz}$           | $\bar{\sigma}_{yz}$            | $\bar{\sigma}_{xy}$ |
|-----|--------------------------|---------------------|-----------|---------------------|---------------------|-------------------------------|--------------------------------|---------------------|
| 2   | Present (12×12)          | HSDT(Q8)            | 21.356    | 2.770               | 0.386               | 0.2174*<br>0.1880+            | 0.1535*<br>0.1317+             | 0.2288              |
|     | Pagano [6]               | Elasticity solution | 21.653    | 2.6530              | 0.3920              | 0.1850                        | 0.1400                         | 0.2340              |
|     | Ramtekkar et al. [41]    | MFEM-3D-LW          | -         | 2.6840              | 0.3960              | 0.1860                        | 0.1420                         | 0.2360              |
|     | Kant et Kommineni [23]   | FEM-Q9-TSDT         | 21.3707   | 2.7985              | -                   | -                             | -                              | 0.2371              |
| 4   | Present (12×12)          | HSDT(Q8)            | 7.1508    | 1.4929              | 0.2375              | 0.279*<br>0.2418+             | 0.1154*<br>0.0997+             | 0.1377              |
|     | Pagano [6]               | Elasticity solution | 7.5962    | 1.5160              | 0.2595              | 0.2390                        | 0.1072                         | 0.1440              |
|     | Ramtekkar et al. [41]    | MFEM-3D-LW          | --        | 1.5700              | 0.2600              | 0.2400                        | 0.108                          | 0.149               |
|     | Wu et Lin [24]           | MFEM-3D-LW          | --        | 1.5480              | 0.2413              | 0.2497                        | --                             | 0.1339              |
|     | Pandya et Kant [21]      | FEM-Q9-HSDT         | 0.6947    | 1.247               | 0.2338              | 0.2382                        | 0.1132                         | 0.1343              |
|     | Manjunatha et Kant [22]  | FEM-Q9-HSDT         | 7.1596    | -                   | --                  | 0.2750                        | 0.1137                         | -                   |
|     | Kant et Kommineni [23]   | FEM-Q9-TSDT         | 7.1502    | 1.4989              | --                  | --                            | --                             | 0.1428              |
|     | Kant et Swaminathan [13] | HSDT                | 7.0551    | 1.5137              | 0.2648              | --                            | --                             | 0.1379              |
|     | IGA [42]                 | TSDT                | 7.0872    | 1.4244              | 0.2361              | 0.2708                        | 0.1169                         | 0.1383              |
|     | IGA [42]                 | HSDT                | 7.0686    | 1.4791              | 0.2391              | 0.3074                        | 0.1274                         | 0.1406              |
| 5   | Present (12×12)          | HSDT(Q8)            | 5.1389    | 1.334               | 0.1955              | 0.299*<br>0.2592 <sup>+</sup> | 0.0986*<br>0.0851 <sup>+</sup> | 0.1149              |
|     | Pagano [6]               | Elasticity solution | 5.4746    | 1.3704              | 0.2094              | 0.2569                        | 0.0918                         | --                  |
|     | Khandelwal et al. [25]   | FEM-Q9-HZZT         | 5.4464    | 1.3617              | 0.2216              | 0.2530                        | 0.1025                         | --                  |
| 10  | Present (12×12)          | HSDT(Q8)            | 2.08426   | 1.1419              | 0.1035              | 0.3454*<br>0.2986+            | 0.05797*<br>0.0493+            | 0.0672              |
|     | Pagano [6]               | Elasticity solution | 2.2004    | 1.1531              | 0.1104              | 0.3000                        | 0.0530                         | 0.0707              |
|     | Pandit et al.[26]        | FEM-Q9-HZZT         | 2.2002    | 1.1483              | 0.1086              | 0.3158                        | 0.0570                         | 0.0709              |
|     | Tu et al.[27]            | FEM-Q9-TSDT         | 2.2027    | 1.1466              | 0.1105              | 0.3181                        | 0.0532                         | 0.0715              |
|     | Khandelwal et al. [25]   | FEM-Q9-HZZT         | 2.1786    | 1.1539              | 0.1184              | 0.3185                        | 0.0598                         | -                   |
|     | Chalak et al.[26]        | FEM-Q9-HZZT         | 2.1775    | 1.1528              | 0.1143              | 0.3058                        | 0.0575                         | 0.0705              |
|     | Ramtekkar et al. [41]    | MFEM-3D-LW          | --        | 1.1590              | 0.1110              | 0.3030                        | 0.0550                         | 0.0720              |
|     | Wu et Lin [24]           | MFEM-3D-LW          | --        | 1.2100              | 0.1115              | 0.3177                        | ----                           | 0.0713              |
|     | Pandya et Kant [21]      | FEM-Q9-HSDT         | 2.023     | 1.110               | 0.1017              | 0.2841                        | 0.05593                        | 0.0666              |
|     | Kant et Kommineni[23]    | FEM-Q9-TSDT         | 2.0864    | 1.1657              | -                   | --                            | --                             | 0.0692              |



|          |                                |                     |         |        |        |                     |                      |        |
|----------|--------------------------------|---------------------|---------|--------|--------|---------------------|----------------------|--------|
|          | Kant et Swaminathan[13]        | HSDT-Anal           | 2.0798  | 1.1523 | 0.1100 | 0.3465              | 0.0538               | 0.0685 |
|          | Nayak et al. [28]              | FEM-Q4-HSDT         | --      | 1.1410 | 0.1034 | 0.3506              | 0.0534               | 0.0685 |
|          | Nayak et al. [28]              | FEM-Q9-HSDT         | --      | 1.1510 | 0.1043 | 0.2815              | 0.0532               | 0.0689 |
|          | IGA [42]                       | TSDT                | 2.0629  | 1.1299 | 0.1028 | 0.3302              | 0.0578               | 0.0679 |
|          | IGA [42]                       | HSDT                | 2.0515  | 1.1424 | 0.1031 | 0.3781              | 0.0628               | 0.0682 |
| 20       | Present (12×12)                | HSDT(Q8)            | 1.1937  | 1.1019 | 0.0678 | 0.3648*<br>0.31374+ | 0.04227*<br>0.03401+ | 0.0493 |
|          | Pagano [6]                     | Elasticity solution | 1.2264  | 1.1100 | 0.0700 | 0.3174              | 0.0361               | 0.0511 |
|          | Pandit et al. [26]             | FEM-Q9-HZZT         | 1.2254  | 1.1055 | 0.0694 | 0.3342              | 0.0392               | 0.0509 |
|          | Khandelwal et al. [25]         | FEM-Q9-HZZT         | 1.2128  | 1.1113 | 0.0769 | 0.3374              | 0.0415               | -      |
|          | Chalak et al.[29]              | FEM-Q9-HZZT         | 1.2121  | 1.1103 | 0.0742 | 0.3272              | 0.0399               | 0.0508 |
|          | Ramtekkar et al. [41]          | MFEM-3D-LW          | --      | 1.1150 | 0.0700 | 0.3170              | 0.0360               | 0.0510 |
|          | Wu et Lin [24]                 | MFEM-3D-LW          | --      | 1.1730 | 0.0724 | 0.3530              | ---                  | 0.0525 |
|          | Kant et Kommineni [23]         | FEM-Q9-HSDT         | 1.1947  | 1.1246 | -      | --                  | --                   | 0.0506 |
|          | Kant et Swaminathan [13]       | HSDT                | 1.1933  | 1.1110 | 0.0705 | --                  | --                   | 0.0504 |
|          | IGA [42]                       | TSDT                | 1.1876  | 1.1027 | 0.0678 | 0.3467              | 0.0408               | 0.0501 |
| IGA [42] | HSDT                           | 1.1850              | 1.1061  | 0.0678 | 0.3974 | 0.0443              | 0.0502               |        |
| 50       | Present (12×12)                | HSDT(Q8)            | 0.92923 | 1.0918 | 0.0563 | 0.3799*<br>0.3147+  | 0.4283*<br>0.02646+  | 0.0435 |
|          | Pagano [6]                     | Elasticity solution | 0.9348  | 1.0990 | 0.0569 | 0.3230              | 0.0306               | 0.0446 |
|          | Pandit et al. [26]             | FEM-Q9-HZZT         | 0.9341  | 1.0948 | 0.0566 | 0.3403              | 0.0333               | 0.0445 |
|          | Chalak et al. [29]             | FEM-Q9-HZZT         | 0.9248  | 1.0997 | 0.0611 | 0.3300              | 0.0321               | 0.0443 |
|          | IGA [42]                       | TSDT                | 0.9284  | 1.0965 | 0.0565 | 0.3520              | 0.0352               | 0.0444 |
|          | IGA [42]                       | HSDT                | 0.9280  | 1.0971 | 0.0565 | 0.4036              | 0.0383               | 0.0445 |
|          | Kant et Kommineni [23]         | FEM-Q9-HSDT         | 0.9299  | 1.1118 | -      | -                   | -                    | 0.0448 |
| 100      | Present (12×12)                | HSDT(Q8)            | 0.8905  | 1.0904 | 0.0546 | 0.4118*<br>0.30167+ | 0.05132*<br>0.02157+ | 0.0427 |
|          | Pagano [6]                     | Elasticity solution | 0.8917  | 1.098  | 0.0550 | 0.324               | 0.0297               | 0.0433 |
|          | Rosalin Sahoo, B.N. Singh [30] | ITZZT-Q8            | 0.8919  | 1.1088 | 0.0555 | 0.3433              | 0.0276               | 0.044  |
|          | Chalak et al.[29]              | HOZT-Q9             | 0.8814  | 1.0982 | 0.0592 | 0.3426              | 0.0332               | 0.0433 |
|          | Pandit et al. [26]             | HOZT-Q9             | 0.8917  | 1.1093 | 0.0547 | 0.3412              | 0.0324               | 0.0434 |
|          | IGA [42]                       | TSDT                | 0.8908  | 1.0957 | 0.0548 | 0.3528              | 0.0344               | 0.0436 |



|                        |             |        |        |        |        |         |        |
|------------------------|-------------|--------|--------|--------|--------|---------|--------|
| IGA [42]               | HSDT        | 0.8907 | 1.0958 | 0.0548 | 0.4046 | 0.0374  | 0.0436 |
| Pandya et Kant [21]    | FEM-Q9-HSDT | 0.891  | 1.108  | 0.0554 | 0.3001 | 0.03362 | 0.044  |
| Kant et Kommineni [23] | FEM-Q9-HSDT | 0.8915 | 1.1058 | -      | -      | -       | 0.044  |

\*Constitutive +Equilibre

Table 3: Normalized transverse displacement, plane stresses, transverse shear stresses of a simply supported sandwich plate ( $0^\circ / C / 0^\circ$ ) under doubly sinusoidal loading.

Through Figs (5, 6, 7, 8, 9, 10,11), the normal  $\bar{\sigma}_{xx}, \bar{\sigma}_{yy}, \bar{\sigma}_{xy}$  and transverse shear  $\bar{\sigma}_{xz}, \bar{\sigma}_{yx}$  stresses states are described through thickness of the sandwich plate in bending behavior for aspect ratios  $a/h=10,4$  according to the constitutive and equilibrium equations. The obtained results stresses are in close agreement with those obtained by Pagano elasticity solution [13] and by TSDT numerical solution [42].

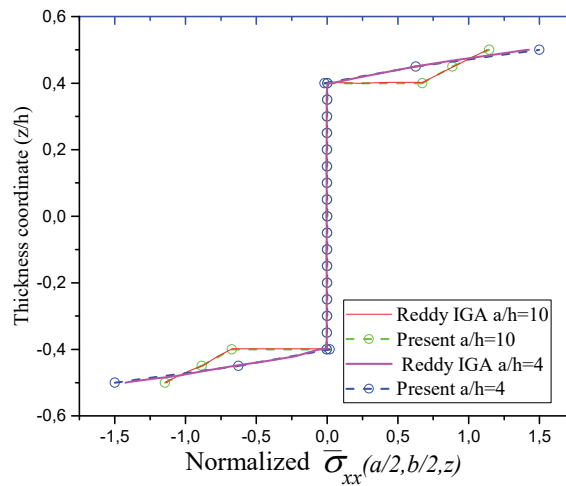


Figure 5: Normal stress distribution  $\bar{\sigma}_{xx}$  through the thickness of a simply supported sandwich plate ( $0^\circ / C / 0^\circ$ ) subject to a sinusoidal load ( $a/b = 10, 4$ ).

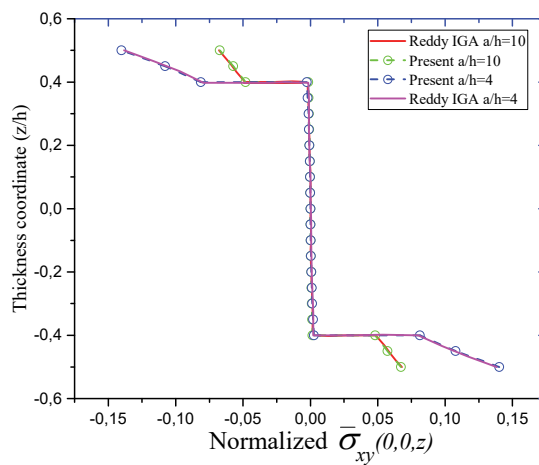


Figure 6: Normal stress distribution  $\bar{\sigma}_{yy}$  through the thickness of a simply supported sandwich plate ( $0^\circ / C / 0^\circ$ ) subject to a sinusoidal load ( $a/h = 10, 4$ ).

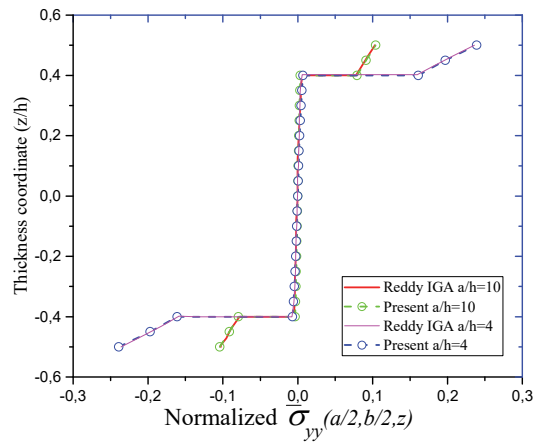


Figure 7: Normal stress distribution  $\bar{\sigma}_{yy}$  through the thickness of a simply supported sandwich plate ( $0^\circ / C / 0^\circ$ ) subject to a sinusoidal load ( $a/h = 10, 4$ ).

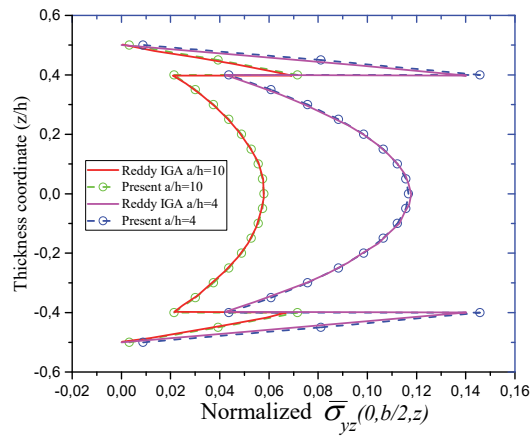


Figure 8: Transverse shear stress distribution  $\bar{\sigma}_{yx}$  through the thickness of a simply supported sandwich plate ( $0^\circ / C / 0^\circ$ ) subject to a sinusoidal load ( $a/h = 10, 4$ ) (Constitutive equations).

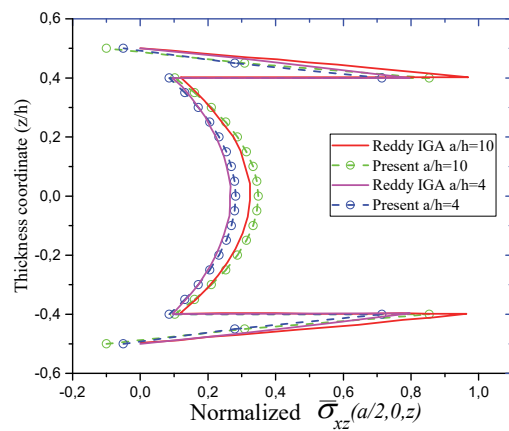


Figure 9: Transverse shear stress distribution  $\bar{\sigma}_{xz}$  through the thickness of a simply supported sandwich plate ( $0^\circ / C / 0^\circ$ ) subject to a sinusoidal load ( $a/h = 10, 4$ ) (Constitutive equations).

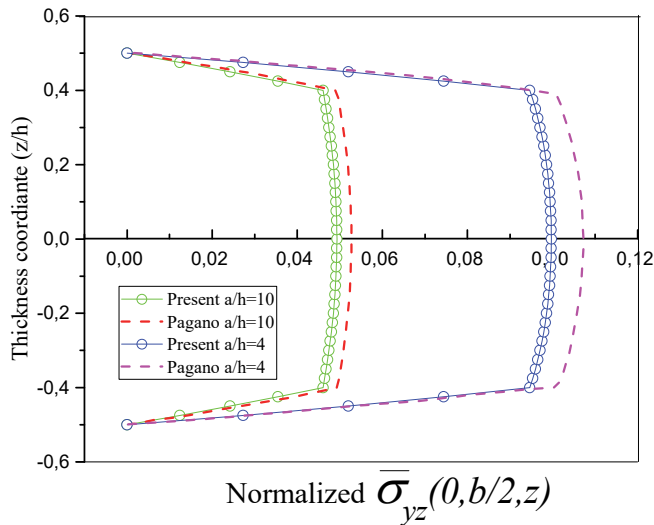


Figure 10: Transverse shear stress distribution  $\bar{\sigma}_{yz}$  through the thickness of a simply supported sandwich plate ( $0^\circ / C / 0^\circ$ ) subject to a sinusoidal load ( $a/h = 10, 4$ ) (Equilibrium equations).

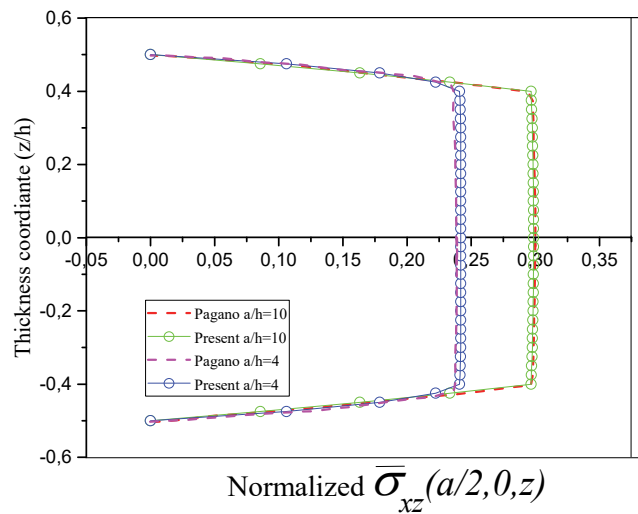


Figure 11: Transverse shear stress distribution  $\bar{\sigma}_{xz}$  through the thickness of a simply supported sandwich plate ( $0^\circ / C / 0^\circ$ ) subject to a sinusoidal load ( $a/h = 10, 4$ ) (Equilibrium equations).

*Three-layer sandwich square plate subject to a uniform load*

In this example, the effect of the scale factor  $R$  ( $\bar{C}_{face} = R\bar{C}_{core}$ ) variation on deflection and stresses state of a simply supported sandwich square plate ( $0^\circ / C / 0^\circ$ ) is studied under a uniform transverse load with aspect ratio  $a/h = 10$  and face and core layers thickness  $hc/hf = 8$ . This sandwich example has been suggested by Srinivas [43]. The material properties of core layer are defined as:

$$\bar{C}_{core} = \begin{bmatrix} 0.999781 & 0.231192 & 0 & 0 & 0 \\ 0.231192 & 0.524886 & 0 & 0 & 0 \\ 0 & 0 & 0.262931 & 0 & 0 \\ 0 & 0 & 0 & 0.26681 & 0 \\ 0 & 0 & 0 & 0 & 0.159914 \end{bmatrix}$$

The normalized deflection and stresses are defined by:

$$\begin{aligned} \bar{w} &= \left( \frac{0.999781w(a/2, b/2, 0)}{q_0b} \right), \bar{\sigma}_{xx}^1 = \left( \frac{\sigma_x^1(a/2, b/2, b/2)}{q_0} \right), \bar{\sigma}_{xx}^2 = \left( \frac{\sigma_x^1(a/2, b/2, 2b/5)}{q_0} \right), \\ \bar{\sigma}_{xx}^3 &= \left( \frac{\sigma_x^2(a/2, b/2, 2b/5)}{q_0} \right), \bar{\sigma}_{yy}^1 = \left( \frac{\sigma_y^1(a/2, b/2, b/2)}{q_0} \right), \bar{\sigma}_{yy}^2 = \left( \frac{\sigma_y^1(a/2, b/2, 2b/5)}{q_0} \right), \\ \bar{\sigma}_{yy}^3 &= \left( \frac{\sigma_y^2(a/2, b/2, 2b/5)}{q_0} \right) \end{aligned}$$

Table 4 shows the deflection and normal stresses solution by the proposed model for different factor scales  $R = 5, 10, 15$  compared with those obtained using the exact solution reported by Srinivas [43], HSDT finite element by Pandya and Kant [21], HSDT meshfree solution by Ferreira et al. [44], TrSDT trigonometric shear deformation theory solution by Mantari



et al. [14] and IHSDT inverse hyperbolic shear deformation theory by Grover et al.[15]. It is noted that the obtained results are in very good correlation with all scale factor R cases when compared with the exact solution.

| R  | Theory                   | $\bar{w}$ | $\bar{\sigma}_{xx}^1$ | $\bar{\sigma}_{xx}^2$ | $\bar{\sigma}_{xx}^3$ | $\bar{\sigma}_{yy}^1$ | $\bar{\sigma}_{yy}^2$ | $\bar{\sigma}_{yy}^3$ |
|----|--------------------------|-----------|-----------------------|-----------------------|-----------------------|-----------------------|-----------------------|-----------------------|
| 5  | Present HSDT(Q8) (12×12) | 257.4323  | 60.1869               | 46.6913               | 9.3382                | 38.3327               | 30.07465              | 6.0149                |
|    | Exact [43]               | 258.97    | 60.353                | 46.623                | 9.34                  | 38.491                | 30.097                | 6.161                 |
|    | FEM-HSDT [21]            | 256.13    | 62.380                | 46.910                | 9.382                 | 38.930                | 30.330                | 6.065                 |
|    | MRBF-HSDT [44]           | 257.110   | 60.366                | 47.003                | 9.401                 | 38.456                | 30.242                | 6.048                 |
|    | CFS-IHSDT [15]           | 255.644   | 60.675                | 47.055                | 9.411                 | 38.522                | 30.206                | 6.041                 |
|    | CFS-TrSDT [14]           | 256.706   | 60.525                | 47.061                | 9.412                 | 38.452                | 30.177                | 6.035                 |
| 10 | Present HSDT(Q8) (12×12) | 155.9531  | 65.3098               | 49.3654               | 4.936                 | 43.2633               | 33.42849              | 3.3428                |
|    | Exact [43]               | 159.38    | 65.332                | 48.857                | 4.903                 | 43.566                | 33.413                | 3.5                   |
|    | FEM-HSDT [21]            | 152.33    | 64.650                | 51.310                | 5.131                 | 42.830                | 33.970                | 3.397                 |
|    | MRBF-HSDT [44]           | 154.658   | 65.381                | 49.973                | 4.997                 | 43.240                | 33.637                | 3.364                 |
|    | CFS-IHSDT [15]           | 154.550   | 65.741                | 49.798                | 4.979                 | 43.4                  | 33.556                | 3.356                 |
|    | CFS-TrSDT [14]           | 155.498   | 65.542                | 49.708                | 4.971                 | 43.385                | 33.591                | 3.359                 |
| 15 | Present HSDT(Q8) (12×12) | 116.9587  | 66.9283               | 49.3353               | 3.289                 | 45.8775               | 34.9577               | 2.3305                |
|    | Exact [43]               | 121.72    | 66.787                | 48.299                | 3.238                 | 46.424                | 34.955                | 2.494                 |
|    | FEM-HSDT [21]            | 110.430   | 66.620                | 51.970                | 3.465                 | 44.920                | 35.410                | 2.361                 |
|    | MRBF-HSDT [44]           | 114.644   | 66.919                | 50.323                | 3.355                 | 45.623                | 35.167                | 2.345                 |
|    | CFS-IHSDT [15]           | 115.820   | 67.272                | 49.813                | 3.321                 | 45.967                | 35.088                | 2.339                 |
|    | CFS-TrSDT [14]           | 115.919   | 67.185                | 49.769                | 3.318                 | 45.910                | 35.081                | 2.339                 |

Table 4: The normalized deflection and stresses of square sandwich plates under uniform load.

An additional analysis is considered for the effect of different scale factors  $R = 5, 10, 15$  on the evolution of in-plane displacements  $u_1(a/2, b/2, z)$ ,  $u_2(a/2, b/2, z)$ , normal stresses  $\bar{\sigma}_{xx}(a/2, b/2, z)$ ,  $\bar{\sigma}_{yy}(a/2, b/2, z)$  and transverse shear stresses  $\bar{\sigma}_{xz}(0, b/2, z)$ ,  $\bar{\sigma}_{yz}(a/2, 0, z)$  with respect to the sandwich plate thickness.

In Fig 12, it is noted for the bending behavior that the in-plane displacements are reduced along the thickness when the scale factor R is increased. In addition, in Figs 13, 14 it can be seen that the normal and transverse shear stresses have also reduced only through the core of plate, whereas they have increased through the faces.



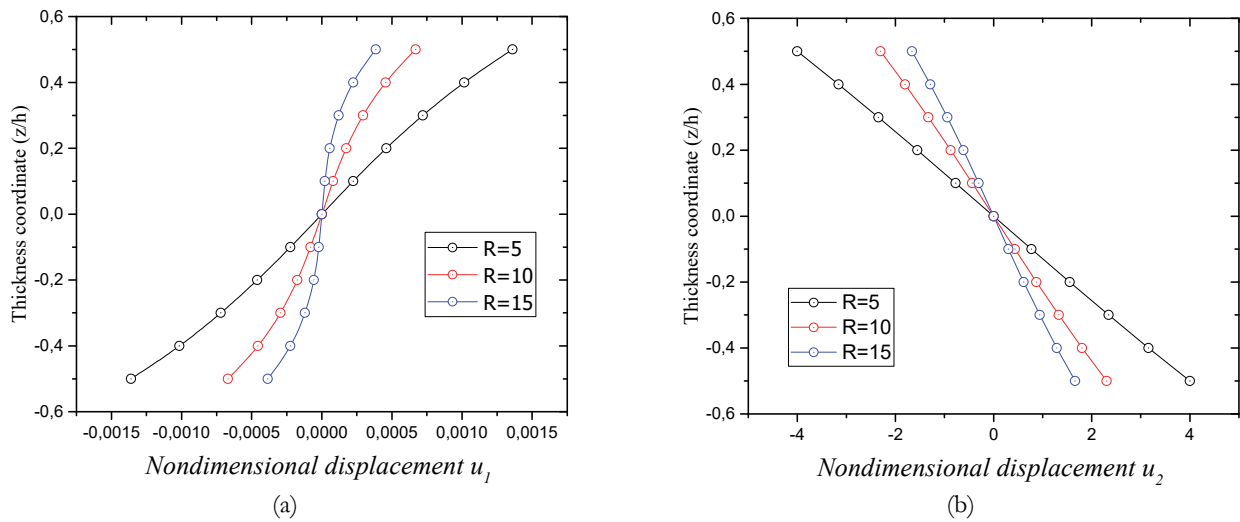


Figure 13: Effect of scale factor R variation on the distribution of normal stresses  $\bar{\sigma}_{xx}$ ,  $\bar{\sigma}_{yy}$  through the thickness of a simply supported  $(0^\circ / C / 0^\circ)$  sandwich plate subject to a uniform transverse load.

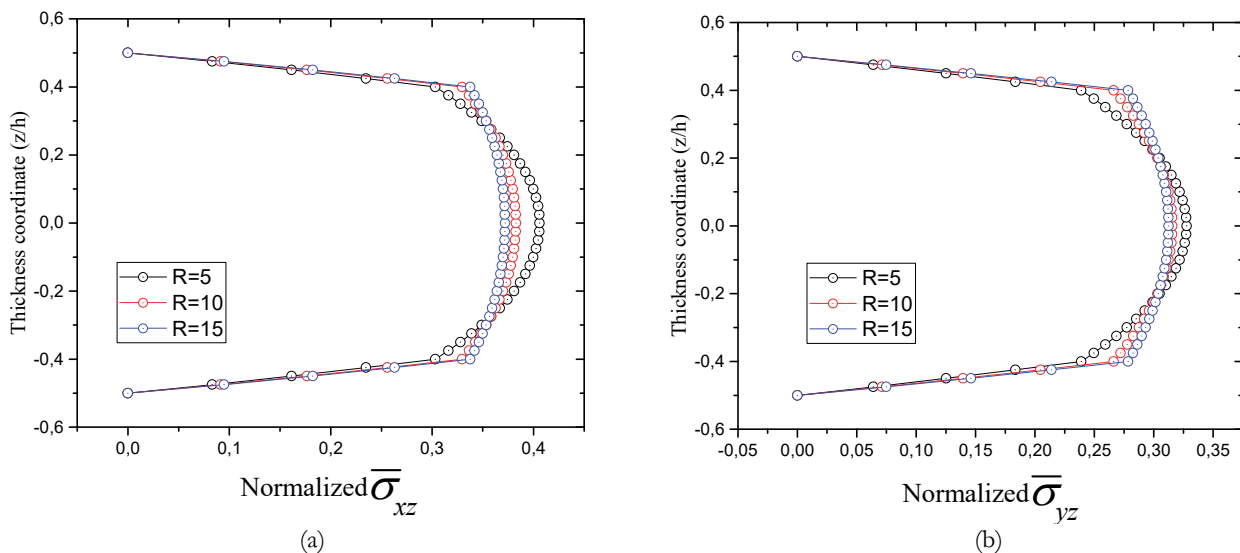


Figure 14: Effect of scale factor R variation on the distribution of transverse shear stresses  $\bar{\sigma}_{xz}$ ,  $\bar{\sigma}_{yz}$  through the thickness of a simply supported  $(0^\circ / C / 0^\circ)$  sandwich plate subject to a uniform transverse load.

### Sandwich Plates with Laminated Face Sheets

In this example, the proposed element is evaluated for different laminated face sheets of rectangular sandwich plates. Kanematsu et al. [16] carried out experimental solution of clamped rectangular sandwich plates (450×300 mm) with four types laminated composite orientation faces SP1, SP2, SP3 and SP4 (Fig. 15). The faces of the sandwiches are symmetrical laminated composite made of carbon/epoxy (Carbon Fiber–Reinforced Plastic-CFRP)  $E_1=105$  GPa,  $E_2=8.74$  GPa,  $G_{12}=G_{13}=G_{23}=4.56$  GPa,  $\nu=0.327$ , while the core is an aluminum honeycomb material (Aluminum Honeycomb Core)  $E_1=68.6$  MPa,  $E_2=68.6$  MPa,  $G_{12}=26.4$  MPa,  $G_{13}=103$  MPa,  $G_{23}=62.1$  MPa,  $\nu=0.3$ . The thickness of each layer is 0.125mm, while the core thickness is 10mm for the SP1 and SP2 types, and 7mm core thickness for the SP3 and SP4 types. The plate is subject to a uniform distributed load of intensity  $q=1.01$  KPa. In addition, the authors provided analytical solutions based on the Rayleigh-Ritz method for the same plate problem, using two types boundary conditions, simply supported (SSSS) and clamped (CCCC). The obtained results of the transverse displacement using the proposed element are given in Table 5, compared with those obtained using analytical solutions and from experimental work given by



Kanematsu et al. [16]. The results have also been compared with those obtained by finite element models of Lee and Fan [45] and Nayak et al. [28], M. O. Belarbi et al. [46]. The comparison results show the reliability and practicality of the proposed element for the studies of laminated faces sandwich structures.

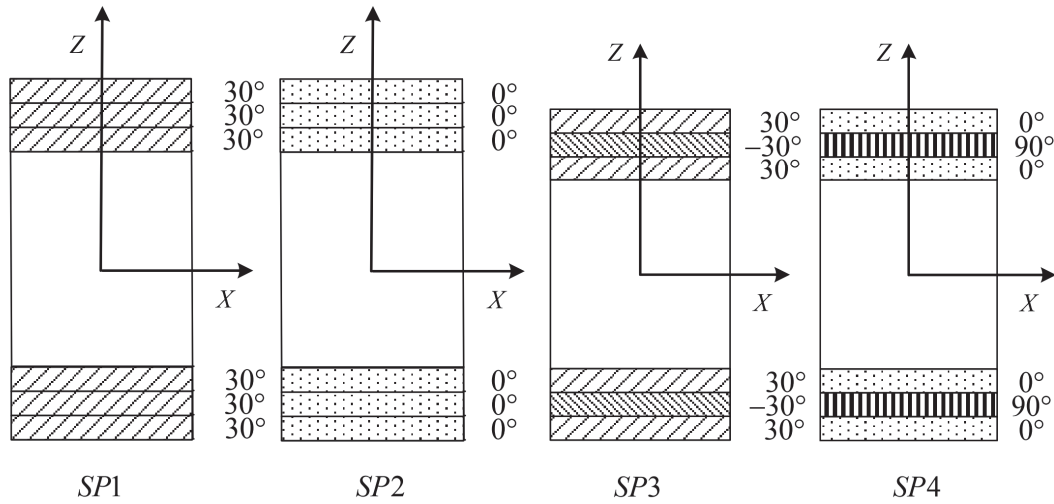


Figure 15: Different types of laminated faces sandwich structures [46]

| References                | Theory                | Central deflection (mm) |          |          |         |
|---------------------------|-----------------------|-------------------------|----------|----------|---------|
|                           |                       | SP1                     | SP2      | SP3      | SP4     |
| Clamped (CCCC)            |                       |                         |          |          |         |
| Present (12×12)           | FEM-Q8-TSDT           | 0.04891                 | 0.056578 | 0.074968 | 0.05469 |
| Kanematsu et al. [16]     | Analytical solution   | 0.05040                 | 0.05400  | 0.07720  | 0.06130 |
| Kanematsu et al. [16]     | Experimental solution | 0.06900                 | 0.08500  | 0.09400  | 0.09000 |
| Lee et Fan [45]           | FEM-Q9-LW             | 0.05190                 | 0.05524  | 0.07834  | 0.06216 |
| Nayak et al. [28]         | FEM-Q9-HSDT           | -                       | 0.05248  | -        | 0.05797 |
| M. O. Belarbi et al. [46] | FEM-Q4-RSFT52         | 0.04906                 | 0.05647  | 0.07506  | 0.05525 |
| Simply supported (SSSS)   |                       |                         |          |          |         |
| Present (12×12)           | FEM-Q8-TSDT           | 0.12124                 | 0.17823  | 0.17213  | 0.2067  |
| Kanematsu et al. [16]     | Analytical solution   | 0.1173                  | 0.1829   | 0.1794   | 0.2206  |
| Lee et Fan [45]           | FEM-Q9-LW             | 0.1213                  | 0.1774   | 0.1729   | 0.2138  |
| Nayak et al. [28]         | FEM-Q9-HSDT           | -                       | 0.1754   | -        | 0.2111  |
| M. O. Belarbi et al. [46] | FEM-Q4-RSFT52         | 0.1160                  | 0.1733   | 0.1695   | 0.2010  |

Table 5: Deflection laminated faces sandwiches plates under uniformly transverse load.



## CONCLUSION

In this paper, an improved  $C^0$  two-dimensional plate finite element (FE) model has been developed for the static analysis of laminated thin and thick sandwich plates. The Reddy's third order shear deformation theory (TSDT) is employed by adopting single layer approach when the warping cross-sectional of in-plane displacements is considered to be cubic for both the face sheets and the core of sandwich. The problem of  $C1$  continuity requirement of the second order derivatives of transverse displacements is circumvented by selecting the degrees of freedom nodal field in an efficient manner. For the present analysis, an eight-node  $C0$  finite element is successfully implemented having seven degrees of freedom for each element node: two displacements ( $u, v$ ) for in-plane behavior and five bending unknowns: a transverse displacement, two rotations and two shear angles ( $w, \psi_x, \psi_y, \theta_x, \theta_y$ ). Whereas element stiffness matrices, which have first order derivative requirement, are solved through a computationally ( $3 \times 3$ ) Gauss integration scheme. In the proposed formulation, there is no stiffness penalty requirement such as: shear correction factors, and numerical techniques to overcome transverse shear locking phenomenon that as used in previous element models. In order to demonstrate the effectiveness and validity of the proposed formulation, many sandwich plates numerical examples are solved and displacements as well as stresses are calculated for different problems and which give results better than other existing 2D finite element models. The results obtained by using the present FE model are successfully compared with those of analytical and numerical solutions available in the literature. The numerical results show that the performance of the present finite element model is excellent in predicting the bending response of thin and thick laminated composites sandwich structures as the error percentage with respect to the 3D elasticity solution is considerably low. The present FE model may, therefore, be recommended for use as accurate tool in other behavior analysis of laminated sandwich plates.

## STATEMENTS AND DECLARATIONS - COMPETING INTERESTS AND FUNDING

The authors declare that they have no known competing financial interests or personal relationships that could have appeared to influence the work reported in this paper.  
There is no funding to declare.

## NOMENCLATURE

|  |  |
|--|--|
| $u_1, u_2, u_3$                                  | Displacement field in the x, y and z directions respectively             |
| $u, v, w$  | Displacement of a point on the mid-plane                                 |
| $\psi_x, \psi_y$                                 | Rotations of normal to the mid-plane about the y and x axes respectively |
| $\theta_x, \theta_y$                             | Shear angles to the mid-plane about the y and x axes respectively        |
| $\epsilon_i$                                     | Strain   |
| $a, b, h$  | Dimensions of the plate along the x, y and z directions respectively     |
| $\sigma_{ij}$                                    | Stress tensor  |
| $[\bar{C}_{ij}]$                                 | Constitutive matrix at the lamina level                                  |
| $E_i$  | Young modulus  |
| $G_{12}, G_{13}, G_{23}$                         | Shears modulus   |
| $\nu_{12}, \nu_{21}$                             | Poisson's ratios   |
| $\{N\}, \{M\}, \{P\}, \{Q\}, \{R\}$              | Resultants forces  |
| $A_{ij}, B_{ij}, D_{ij}, E_{ij}, F_{ij}, H_{ij}$ | Extensional, coupling and flexural stiffnesses                           |
| $A_{ij}^S, D_{ij}^S, F_{ij}^S$                   | Transverse shear stiffnesses   |



|  |   |
|--|---|
| $\bar{N}_i$  | Interpolation functions                             |
| $[B_\varepsilon^0], [B_\kappa^0], [B_\kappa^2], [B_\varepsilon^s], [B_\kappa^s]$ | Strain displacement matrices                        |
| $\{\delta\}$   | Element nodal field variables                       |
| $\{F\}$  | Element load vector                                 |
| $[K]_e$  | Element stiffness matrix                            |
| $b_c, b_f$   | Core and face thicknesses of sandwich, respectively |

## REFERENCES

- [1] Kirchhoff, G. (1850). Über das Gleichgewicht und die Bewegung einer elastischen Scheibe, *Journal für die reine und angewandte Mathematik (Crelles Journal)*, 1850 (40), pp. 51-88. DOI: 10.1515/crll.1850.40.51
- [2] Reddy, J.N. (2004). *Mechanics of laminated composite plates and shells: theory and analysis*, CRC press.
- [3] Reissner, E. (1945). The effect of transverse shear deformations on the bending of elastic plates, *Journal of Applied Mechanics*, 12 pp. A69-A77. DOI: <https://doi.org/10.1115/1.4009435>
- [4] Whitney, J.M. (1969). The Effect of Transverse Shear Deformation on the Bending of Laminated Plates, *Journal of Composite Materials*, 3 (3), pp. 534-547. DOI: 10.1177/002199836900300316
- [5] Carrera, E. (2002). Theories and finite elements for multilayered, anisotropic, composite plates and shells, *Archives of Computational Methods in Engineering*, 9 (2), pp. 87-140. DOI: 10.1007/BF02736649
- [6] Pagano, N. (1970). Exact solutions for rectangular bidirectional composites and sandwich plates, *Journal of Composite Materials*, 4 (1), pp. 20-34. DOI: 10.1177/002199837000400102
- [7] Reddy, J. , Robbins, D. (1994). Theories and computational models for composite laminates, *Applied Mechanics Reviews*, 47 (6), pp. 147-169. DOI: 10.1115/1.3111076
- [8] Ghugal, Y. , Shimpi, R. (2002). A review of refined shear deformation theories of isotropic and anisotropic laminated plates, *Journal of Reinforced Plastics and Composites*, 21 (9), pp. 775-813. DOI: 10.1177/073168402128988481
- [9] Reddy, J.N. (1984). A simple higher-order theory for laminated composite plates, *Journal of Applied Mechanics*, 51 (4), pp. 745-752. DOI: 10.1115/1.3167719
- [10] Reddy, J.N. (1984(c)). A refined nonlinear theory of plates with transverse shear deformation, *International Journal of Solids and Structures*, 20 (9), pp. 881-896. DOI: 10.1016/0020-7683(84)90056-8
- [11] Barut, A., Madenci, E., Heinrich, J., Tessler, A. (2001). Analysis of thick sandwich construction by a {3,2}-order theory, *International Journal of Solids and Structures*, 38 (34), pp. 6063-6077. DOI: 10.1016/S0020-7683(00)00367-X
- [12] Noor, A.K., Burton, W.S., Bert, C.W. (1996). Computational Models for Sandwich Panels and Shells, *Applied Mechanics Reviews*, 49 (3), pp. 155-199. DOI: 10.1115/1.3101923
- [13] Kant, T. , Swaminathan, K. (2002). Analytical solutions for the static analysis of laminated composite and sandwich plates based on a higher order refined theory, *Composite structures*, 56 (4), pp. 329-344. DOI: 10.1016/S0263-8223(02)00017-X
- [14] Mantari, J., Oktem, A., Soares, C.G. (2012). A new trigonometric shear deformation theory for isotropic, laminated composite and sandwich plates, *International Journal of Solids and Structures*, 49 (1), pp. 43-53. DOI: 10.1016/j.ijsolstr.2011.09.008
- [15] Grover, N., Maiti, D., Singh, B. (2013). A new inverse hyperbolic shear deformation theory for static and buckling analysis of laminated composite and sandwich plates, *Composite Structures*, 95 pp. 667-675. DOI: 10.1016/j.compstruct.2012.08.012
- [16] Kanematsu, H.H., Hirano, Y., Iyama, H. (1988). Bending and vibration of CFRP-faced rectangular sandwich plates, *Composite Structures*, 10 (2), pp. 145-163. DOI: 10.1016/0263-8223(88)90044-X
- [17] Torabizadeh, M.A., Fereidoon, A. (2021). Applying Taguchi Approach to Design Optimized Effective Parameters of Aluminum Foam Sandwich Panels Under Low-Velocity Impact, *Iranian Journal of Science and Technology, Transactions of Mechanical Engineering*, pp. DOI: 10.1007/s40997-021-00441-5
- [18] Marino, M., Nerilli, F., Vairo, G. (2014). A finite-element approach for the analysis of pin-bearing failure of composite laminates, *Frattura ed Integrità Strutturale*, 8 (29), pp. 241-250. DOI: 10.3221/IGF-ESIS.29.21
- [19] Delioui, A., Bouchouicha, B. (2018). Fatigue crack propagation in welded joints X70, *Frattura ed Integrità Strutturale*, 12 (46), pp. 306-318. DOI: 10.3221/igf-esis.46.28



- [20] Zhang, Y., Yang, C. (2009). Recent developments in finite element analysis for laminated composite plates, *Composite Structures*, 88 (1), pp. 147-157. DOI: 10.1016/j.compstruct.2008.02.014
- [21] Pandya, B. , Kant, T. (1988). Higher-order shear deformable theories for flexure of sandwich plates-finite element evaluations, *International Journal of Solids and Structures*, 24 (12), pp. 1267-1286. DOI: 10.1016/0020-7683(88)90090-X
- [22] Manjunatha, B.S. , Kant, T. (1993). On evaluation of transverse stresses in layered symmetric composite and sandwich laminates under flexure, *Engineering computations*, 10 (6), pp. 499-518. DOI: 10.1108/eb023922
- [23] Kant, T. , Kommineni, J. (1992). C 0 finite element geometrically non-linear analysis of fibre reinforced composite and sandwich laminates based on a higher-order theory, *Computers & structures*, 45 (3), pp. 511-520. DOI: [https://doi.org/10.1016/0045-7949\(92\)90436-4](https://doi.org/10.1016/0045-7949(92)90436-4)
- [24] Wu, C.-P., Lin, C.-C. (1993). Analysis of sandwich plates using a mixed finite element, *Composite Structures*, 25 (1), pp. 397-405. DOI: 10.1016/0263-8223(93)90187-U
- [25] Khandelwal, R.P., Chakrabarti, A., Bhargava, P. (2013). An efficient FE model based on combined theory for the analysis of soft core sandwich plate, *Computational Mechanics*, 51 (5), pp. 673-697. DOI: 10.1007/s00466-012-0745-3
- [26] Pandit, M.K., Sheikh, A.H., Singh, B.N. (2008). An improved higher order zigzag theory for the static analysis of laminated sandwich plate with soft core, *Finite Elements in Analysis and Design*, 44 (9-10), pp. 602-610. DOI: 10.1016/j.finel.2008.02.001
- [27] Tu, T.M., Quoc, T.H. (2010). Finite element modeling for bending and vibration analysis of laminated and sandwich composite plates based on higher-order theory, *Computational Materials Science*, 49 (4), pp. S390-S394. DOI: 10.1016/j.commatsci.2010.03.045
- [28] Nayak, A., Moy, S.J., Sheno, R. (2003). Quadrilateral finite elements for multilayer sandwich plates, *The Journal of Strain Analysis for Engineering Design*, 38 (5), pp. 377-392. DOI: 10.1243/00131644JST.2003.38.5.377
- [29] Chalak, H.D., Chakrabarti, A., Iqbal, M.A., Hamid Sheikh, A. (2012). An improved C0 FE model for the analysis of laminated sandwich plate with soft core, *Finite Elements in Analysis and Design*, 56 pp. 20-31. DOI: 10.1016/j.finel.2012.02.005
- [30] Sahoo, R., Singh, B. (2013). A new shear deformation theory for the static analysis of laminated composite and sandwich plates, *International Journal of Mechanical Sciences*, 75 pp. 324-336. DOI: 10.1016/j.ijmecsci.2013.08.002
- [31] Batoz, J.L., Tahar, M.B. (1982). Evaluation of a new quadrilateral thin plate bending element, *International Journal for Numerical Methods in Engineering*, 18 (11), pp. 1655-1677. DOI: 10.1002/nme.1620181106
- [32] Reddy, J.N. (1989). On refined computational models of composite laminates, *International Journal for Numerical Methods in Engineering*, 27 (2), pp. 361-382. DOI: 10.1002/nme.1620270210
- [33] Phan, N. , Reddy, J. (1985). Analysis of laminated composite plates using a higher-order shear deformation theory, *International Journal for Numerical Methods in Engineering*, 21 (12), pp. 2201-2219. DOI: 10.1002/nme.1620211207
- [34] Averill, R. , Reddy, J. (1992). An assessment of four-noded plate finite elements based on a generalized third-order theory, *International Journal for Numerical Methods in Engineering*, 33 (8), pp. 1553-1572. DOI: 10.1002/nme.1620330802
- [35] Ren, J. , Hinton, E. (1986). The finite element analysis of homogeneous and laminated composite plates using a simple higher order theory, *Communications in Applied Numerical Methods*, 2 (2), pp. 217-228. DOI: 10.1002/cnm.1630020214
- [36] Liu, I.-W. (1996). An element for static, vibration and buckling analysis of thick laminated plates, *Computers & structures*, 59 (6), pp. 1051-1058. DOI: 10.1016/0045-7949(95)00350-9
- [37] Belkaid, K. (2019). Development of a 2D isoparametric finite-element model based on reddy's third-order theory for the bending behavior analysis of composite laminated plates, *Mechanics of Composite Materials*, 55 (2), pp. 241-258. DOI: 10.1007/s11029-019-09807-y
- [38] Belkaid, K. (2019). Buckling Analysis of Isotropic and Composite Laminated Plates: New Finite Element Formulation. in *Computational Methods and Experimental Testing In Mechanical Engineering of Conference*. Springer. DOI: 10.1007/978-3-030-11827-3\_8
- [39] Zienkiewicz, O.C., Cheung, Y.K. (1964). The finite element method for analysis of elastic isotropic and orthotropic slabs. in *ICE Proceedings of Conference*. Thomas Telford.
- [40] Hughes, T.J., Cohen, M., Haroun, M. (1978). Reduced and selective integration techniques in the finite element analysis of plates, *Nuclear Engineering and Design*, 46 (1), pp. 203-222. DOI: 10.1016/0029-5493(78)90184-X
- [41] Ramtekkar, G., Desai, Y., Shah, A. (2003). Application of a three-dimensional mixed finite element model to the flexure of sandwich plate, *Computers & structures*, 81 (22-23), pp. 2183-2198. DOI: 10.1016/S0045-7949(03)00289-X



- [42] Nguyen-Xuan, H., Thai, C.H., Nguyen-Thoi, T. (2013). Isogeometric finite element analysis of composite sandwich plates using a higher order shear deformation theory, *Composites Part B: Engineering*, 55 pp. 558-574.  
DOI: 10.1016/j.compositesb.2013.06.044
- [43] Srinivas, S. (1973). A refined analysis of composite laminates, *Journal of Sound and Vibration*, 30 (4), pp. 495-507.  
DOI: 10.1016/S0022-460X(73)80170-1
- [44] Ferreira, A.J.M., Roque, C.M.C., Martins, P.A.L.S. (2003). Analysis of composite plates using higher-order shear deformation theory and a finite point formulation based on the multiquadric radial basis function method, *Composites Part B: Engineering*, 34 (7), pp. 627-636. DOI: 10.1016/S1359-8368(03)00083-0
- [45] Lee, L.J., Fan, Y.J. (1996). Bending and vibration analysis of composite sandwich plates, *Computers & structures*, 60 (1), pp. 103-112. DOI: 10.1016/0045-7949(95)00357-6
- [46] Belarbi, M., Tati, A. (2016). Bending analysis of composite sandwich plates with laminated face sheets: new finite element formulation, *Journal of Solid Mechanics* 8 (2), pp. 280-299.